Available online at www.sciencedirect.com
SCIENCE DIRECT
Solid State Ionics 177 (2006) 53 – 58
SOLID STATE IONICS
www.elsevier.com/locate/ssi

An analytical solution to Li/Li^+ insertion into a porous electrode

Shengyi Liu

Department of Electrical Engineering, University of South Carolina, Columbia, SC 29208, United States

Received 18 May 2005; received in revised form 18 August 2005; accepted 30 September 2005

Abstract

The dynamic faradic properties of the lithium ion batteries are primarily determined by the process of lithium ion insertion into a porous electrode. In this paper, we present an analytical result of the intercalating process of Li/Li^+ into a spherical particle of graphite or cobalt oxide immersed in a conductive electrolyte. Using the finite integral transform method, an exact solution to the concentration profile was obtained for arbitrary linear initial and boundary conditions. To avoid analytical difficulties with respect to the boundary conditions of second kind, the method of pseudo-steady-state is applied. The final solution uniformly converges, and can be used for accurate and fast dynamic modelling and simulation.

Keywords: Diffusion; Intercalation; Lithium ion; Finite integral transform; Porous electrode; Psuedo steady state

1. Introduction

The motivation of this work is to develop a chemical-principle-based model for the lithium ion (Li^+) battery to ensure its fidelity and entirety without compromising the computation speed, so that the model can be used not only for behaviour characterization, but also for life cycle prediction and design optimization in a complex system. Advanced numerical algorithms, such as the finite element method (FEM) and the finite difference method (FDM), allow results of a high accuracy. However, they demand extensive computing time. On the other hand, models based on empirical formula or data regressions offer advantages of simple and fast evaluation, but they fall short in terms of providing a physical insight of the electrochemical activities, and hence are deficient of trustworthiness.

The full scale Li^+ battery model is essentially based on the concentrated solution and porous electrode theories [1]. One representative work is that by Doyle [2,3], in which the behaviour of the battery in terms of one dimensional concentration and potential distributions are governed by a group of boundary-value problems (BVPs). In this model, the micropore-structured electrode is treated as a continuum with the Bruggeman characterization of binary constituents [4], whereas the local surface concentration of Li^+ at a micro spherical granule of graphite immersed in a conductive electrolyte, where the Butler-Volmer reaction is assumed dominant, is determined from the diffusion process. Thus, the treatment for the surface concentration at an isolated granule is of discrete nature. This continuous-discrete description is currently used as a base model for further investigations of many Li^+ battery properties, for example, the temperature effect by incorporating thermal transport properties [5], the cycle life modelling by considering capacity fade mechanisms [6,7].

There are a large number of unknowns to solve from Doyle's model. The number of unknowns is greatly multiplied when they are localized at the nodes of mesh divisions if the spatial-mesh-based FEM or FDM is used, which exacerbates the computation effort. One approach to avoid time-consuming spatial calculation is to use the finite integral transform (FIT) [8] to eliminate analytically the independent spatial variables from the partial differential equations, and to generate a first-order differential equation in terms of time only, to which an analytical solution can be easily found. The remaining problem is a group of coupled algebraic equations concerning the time-varying potentials and concentrations at the points of interest that can be used to construct a model for efficient computer simulation.

A systematic application of the FIT method to the diffusion BVPs with time-dependent sources and boundary conditions of all three kinds is mainly dedicated to the work by Ölçer [9,10].

E-mail address: liusville@gmail.com.

0167-2738/$ - see front matter © 2005 Elsevier B.V. All rights reserved.
doi:10.1016/j.ssi.2005.09.053

In his work, Ölçer proposed an approach for the solution comprising pseudo-steady states (PSS) and transients to guarantee a uniform convergence of the solution. To our best knowledge, Ölçer's approach has not been used for the Li^+ battery systems. Presented in this paper is the FIT analysis of the Li intercalation into a spherical particle of granular graphite immersed in a conductive electrolyte (similarly the Li^+ intercalation in a cobalt oxide particle), which is part of our effort to model the lithium ion battery using Ölçer's approach.

2. Problem description

The intercalating process of Li in a spherical carbon particle (similarly for Li^+ in a cobalt oxide particle) immersed in a conductive electrolyte, following Doyle's notations, is given as the following BVP on a finite region of $\Omega \in R^3$,

$$\begin{cases} \dfrac{1}{r^2}\dfrac{\partial}{\partial r}\left(r^2\dfrac{\partial c(r,t)}{\partial r}\right)+\dfrac{g(r,t)}{D}=\dfrac{1}{D}\dfrac{\partial c(r,t)}{\partial t}, & 0<r<R_o, t>0,\\ \dfrac{\partial c(r,t)}{\partial r}=0, & r=0, t>0,\\ \dfrac{\partial c(r,t)}{\partial r}=-\dfrac{1}{D}j_n(t), & r=R_o, t>0,\\ c(r,0)=c_0, & 0\le r\le R_o, t=0. \end{cases} \tag{1}$$

where the diffusion coefficient is assumed constant, and the concentration within the sphere is independent of azimuthal angle θ and zenithal angle ϕ. For generality, we allow the source term, the boundary conditions, to have arbitrary function forms. The BVP (1) can be converted to (2) for a matter of convenience:

$$\begin{cases} \dfrac{1}{\rho^2}\dfrac{\partial}{\partial \rho}\left(\rho^2\dfrac{\partial \chi(\rho,\tau)}{\partial \rho}\right)+\dfrac{g(\rho,\tau)}{D}=\dfrac{\partial \chi(\rho,\tau)}{\partial \tau}, & 0<\rho<1, \tau>0,\\ \dfrac{\partial \chi(\rho,\tau)}{\partial \rho}=0, & \rho=0, \tau>0,\\ \dfrac{\partial \chi(\rho,\tau)}{\partial \rho}=-\dfrac{R_o}{D}j_n(\tau), & \rho=1, \tau>0,\\ \chi(\rho,\tau)=0, & 0\le\rho\le 1, \tau=0. \end{cases} \tag{2}$$

where we have defined,

$$\begin{cases} \chi(\rho,\tau)=c(r,t)-c(r,0),\\ \rho=r/R_o,\\ \tau=\left(D/R_o^2\right)\cdot t. \end{cases} \tag{3}$$

Thus, a Sturm-Liouville problem corresponding to (2) is,

$$\begin{cases} \dfrac{1}{\rho^2}\dfrac{d}{d\rho}\left(\rho^2\dfrac{d\psi_m}{d\rho}\right)=-\lambda_m^2\psi_m, & 0<\rho<1,\\ \dfrac{d\psi_m}{d\rho}=0, & \rho=0,\\ \dfrac{d\psi_m}{d\rho}=0, & \rho=1. \end{cases} \tag{4}$$

The eigen functions that satisfy (4) are given as,

$$\psi_m(\rho)=\frac{\sin(\lambda_m\rho)}{\rho}, \tag{5}$$

Table 1
First 20 roots of $\tan(\lambda_m)=\lambda_m$

m	λ_m	m	λ_m
1	4.4934	11	36.1006
2	7.7253	12	39.2444
3	10.9041	13	42.3879
4	14.0662	14	45.5311
5	17.2208	15	48.6744
6	20.3713	16	51.8170
7	23.5195	17	54.9597
8	26.6661	18	58.1023
9	29.8116	19	61.2447
10	32.9564	20	64.3871

where λ_m is determined from the following eigen value equation, taking some discrete values only (see Table 1).

$$\tan(\lambda_m)=\lambda_m. \tag{6}$$

Since the boundary conditions in problem (2) are of second kind, the convergence of the result from a usual FIT procedure can not be guaranteed [8]. Therefore, in the following we seek the solution using Ölçer's PSS approach.

3. Solution

A general solution to problem (2) given by Ölçer takes a form of:

$$\begin{aligned} \chi(\rho,\tau)=&\frac{1}{V}\int_V\chi(\rho,0)dv+\sum_{j=0}^{q}\left[\Omega_j(\tau)+\chi_{0j}(\rho,\tau)\right]\\ &+\sum_{m=1}^{\infty}A_m\psi_m(\rho)e^{-\lambda_m^2\tau}\cdot\\ &\times\left\{\int_V\psi_m(\rho)\left[\chi(\rho,0)-\sum_{j=0}^{q}\chi_{0j}(\rho,0)\right]dv\right.\\ &\left.-\sum_{j=0}^{q}\left[\int_0^{\tau}\left[e^{\lambda_m^2\tau}\int_V\psi_m(\rho)\frac{\partial\chi_{0j}(\rho,\tau)}{\partial\tau}dv\right]d\tau\right]\right\}, \end{aligned} \tag{7}$$

where $\Omega_j(\tau)$ is defined as,

$$\begin{aligned} \Omega_j(\tau)=&\frac{1}{V}\left[\delta_{oj}\int_0^{\tau}\int_V g(\rho,\tau)\frac{R_o^2}{D}dvd\tau\right.\\ &\left.+\delta_{ij}\int_0^{\tau}\int_{S_i}\left(\frac{\partial\chi_{0,j}}{\partial\rho}\right)_{S_i}R_o ds_i d\tau\right], \end{aligned} \tag{8}$$

where δ is the Kronecker operator,

$$\delta_{ij}=\begin{cases} 0, & i\neq j,\\ 1, & i=j. \end{cases} \tag{9}$$

and $i=1, 2, \ldots, q$, $j=0, 1, \ldots, q$.

$\chi_{0j}(\rho,\tau)$ in (7) and (8) are called the zero-order pseudo-steady state concentration distributions, and are sought from the following auxiliary BVPs:

$$\begin{cases} \dfrac{1}{\rho^2}\dfrac{\partial}{\partial\rho}\left(\rho^2\dfrac{\partial\chi_{0j}(\rho,\tau)}{\partial\rho}\right)+\delta_{0j}\dfrac{R_o^2}{D}g(\rho,\tau)=\dfrac{d\Omega_j(\tau)}{d\tau}, & 0<\rho<1,\\ \dfrac{D}{R_0}\dfrac{\partial\chi_{0j}(\rho,\tau)}{\partial\rho}=\delta_{ij}f_i(S_i,\tau), & \rho\epsilon S_i, i=1,2,\ldots q. \end{cases} \tag{10}$$

Clearly, the eigen functions of (10) are also defined by (4). Eq. (9) and BVPs (10) indicate that the pseudo-steady state concentrations are the results either from the internal source, or from each of the boundary conditions. To uniquely determine the pseudo-steady states, it is required that,

$$\int_V \chi_{0j}(\rho,\tau)dv = 0. \tag{11}$$

The norm appeared in (7) can be found according to,

$$A_m = \frac{1}{\int_V \psi_m^2(\rho)dv} = \frac{1+\lambda_m^2}{2\pi\lambda_m^2} \tag{12}$$

Applying (8) to problem (2), we can find,

$$\begin{cases} \Omega_0(\tau) = 0 \\ \Omega_1(\tau) = 0 \\ \Omega_2(\tau) = -\dfrac{3R_o}{D}\displaystyle\int_0^\tau j_n(\tau)d\tau \end{cases} \tag{13}$$

From (10) and (11), the pseudo-steady states can be found as:

$$\begin{cases} \chi_{00}(\rho,\tau) = 0 \\ \chi_{01}(\rho,\tau) = 0 \\ \chi_{02}(\rho,\tau) = \dfrac{R_o}{2D}j_n(\tau)\left[\dfrac{3}{5}-\rho^2\right] \end{cases} \tag{14}$$

Notice that in obtaining (13) and (14), we have set $g(\rho,\tau)=0$ based on the nature of a graphite particle (no Li can be generated from graphite). Now using (12)–(14) in (7), we reach a solution to the BVP (2):

$$\begin{aligned} \chi(\rho,\tau) = & -\frac{3R_o}{D}\int_0^\tau j_n(\tau)d\tau + \frac{R_o}{2D}j_n(\tau)\left[\frac{3}{5}-\rho^2\right] \\ & + \frac{2R_o}{D}\sum_{m=1}^{\infty}\frac{\sqrt{1+\lambda_m^2}}{\lambda_m^3}\frac{\sin(\lambda_m\rho)}{\rho}e^{-\lambda_m^2\tau} \\ & \times\left[e^{\lambda_m^2\tau}j_n(\tau) - \lambda_m^2\int_0^\tau e^{\lambda_m^2\tau}j_n(\tau)d\tau\right] \end{aligned} \tag{15}$$

The solution to BVP (1), using backward conversion of (3), can then be found as:

$$\begin{aligned} c(r,t) = & c_0 - \frac{3}{R_o}\int_0^t j_n(t)dt + \frac{R_o}{2D}j_n(t)\left[\frac{3}{5}-(r/R_o)^2\right] + \frac{2R_o}{D} \\ & \times\sum_{m=1}^{\infty}\frac{\sqrt{1+\lambda_m^2}}{\lambda_m^3}\frac{\sin(\lambda_m r/R_o)}{r/R_o}e^{-\lambda_m^2 Dt/R_o^2} \\ & \times\left[e^{\lambda_m^2 Dt/R_o^2}j_n(t) - \frac{\lambda_m^2 D}{R_o^2}\int_0^t e^{\lambda_m^2 Dt/R_o^2}j_n(t)dt\right] \end{aligned} \tag{16}$$

4. Application examples

To verify the correctness of Eq. (16), we consider first a simple application example.

Assuming that the intercalation undergoes a constant and uniform Li flux on the surface of a spherical carbon granule, as shown in Fig. 1. That is,

$$j_n(t) = -J_0\left(\text{moles/m}^2/\text{s}\right), \tag{17}$$

where the negative sign indicates the flux is directed into the sphere and opposes the radial direction. Applying (17) in (16), the solution reduces to,

$$\begin{aligned} c(r,t) = & c_0 + \frac{3J_0 t}{R_o} - \frac{J_0\left(3R_o^2-5r^2\right)}{10DR_o} - \frac{2R_oJ_o}{D} \\ & \times\sum_{m=1}^{\infty}\frac{\sqrt{1+\lambda_m^2}}{\lambda_m^3}\frac{\sin(\lambda_m r/R_o)}{r/R_o}e^{-\lambda_m^2 Dt/R_o^2} \end{aligned} \tag{18}$$

This is the exact result obtained by Carslaw and Jaeger [11] for a prescribed surface flux into the sphere. This indicates that Eq. (16) is correct and is a more generalized result.

To apply (18) to the Li/Li$^+$ intercalation process, one should bear in mind that the theoretical result of (18) is subject to physical limitations, otherwise the result is meaningless. The first of these limitations comes from the fact that the diffusion of Li or Li$^+$ takes a finite time. Like the wave front for wave propagation, we use the diffusion front for a diffusion process, which is defined as the position in the sphere at which the first Li atom or ion arrives. Beyond the front, the concentration is zero (Eq. (18) yields negative concentration within this region. Therefore, it does not apply); from the surface to the front, the concentration follows (18). To characterize the diffusion front, we use the concept of the diffusion velocity (also called the mean velocity) [12], which can be found according to:

$$v_d = -D\frac{\nabla c}{c} \tag{19}$$

As expected, the diffusion velocity depends on the concentration gradient, and it is in general a function of

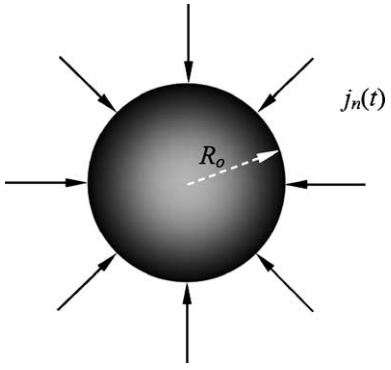

Fig. 1. Uniform Li flux into a spherical carbon granule.

position and time. To a first approximation, we estimate the average diffusion velocity using the value at the beginning of time and on the surface of the sphere. It yields,

$$v_d(R_o,0) = -D\frac{5}{R_o\left(1-10\sum_{m=1}^{\infty}\frac{1}{\lambda_m^2}\right)} \quad (20)$$

where the negative sign indicates an inward direction. For $D=2.6\times10^{-10}$ m^2/s, and $R_o=3.5\times10^{-6}$ m, the diffusion velocity at the surface and at the time of zero second is found to be -6.861×10^{-4} m/s. The estimated time for a first atom to arrive the center of the sphere, using the above velocity as an average one, is thus about 5.1 ms. This estimation gives us a rough idea about the diffusion velocity within the carbon granule.

The second physical limitation is due to a finite density of intercalation sites within the graphite, which is determined by the molecular structure of carbon granule in the porous electrode. Thus there exists a maximum or saturation Li intercalation density.

Considering these limitations, Eq. (18) can be used to plot the concentration profiles as a function of position and time within the sphere.

Fig. 2 shows that concentration profiles as a function of position and parameterized using the time. From this figure, we can clearly see the position of the diffusion front. At 10 μs, the front penetrates to the position of 2.4 μm. The front reaches the center of the sphere between 5.4 ms and 5.5 ms, which is within the same order of magnitude estimated according to Eq. (20). After about 10 ms, the concentration is nearly uniform everywhere in the granule and increases linearly with time.

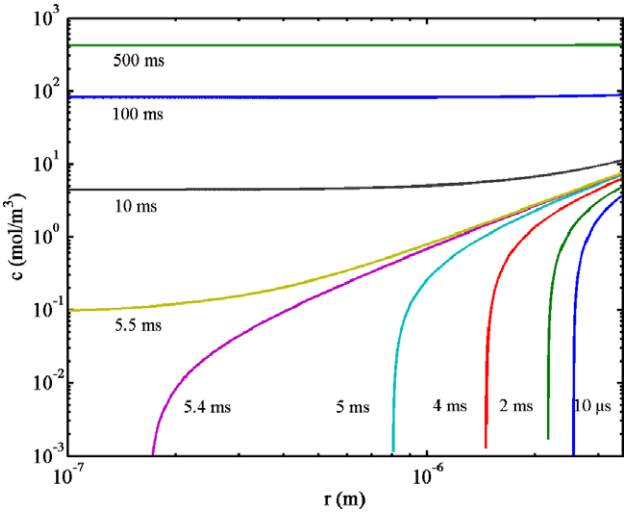

Fig. 2. Li/Li$^+$ concentration distribution under a uniform and constant surface flux density injection. $J_o=0.001$ moles/m^2/s, $c_o=0$ moles/m^3.

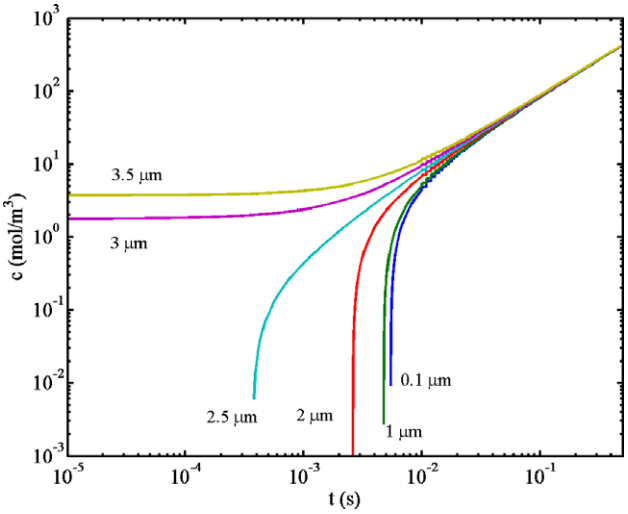

Fig. 3. Li/Li$^+$concentration profile under a uniform and constant surface flux density injection. $J_o=0.001$ moles/m^2/s, $c_o=0$ moles/m^3.

Fig. 3 shows the concentration profiles as a function of time and parameterized using the position. As can be seen, at 0.1 μm from the center, there is no intercalation until about 5.5 ms, while at 2.5 μm from the center, intercalation occurs at about 0.4 ms. At the surface, the concentration is the highest. Again after about 10 ms, the concentration becomes uniform and linearly increases with the time. To further view the spatial- and temporal-evolution of the concentration within the sphere, the 3D plot of Eq. (18) is shown in Fig. 4, which of course confirms again the conclusions drawn from Figs. 2 and 3: the concentration progressively increasing from the surface to the center; no intercalation at the center until about 5.5 ms; and the concentration is nearly uniform throughout the sphere after 10 ms.

Next, we consider a more general application example—a time-varying boundary condition. The surface flux density is of a sinusoidal function form, as practically the battery is

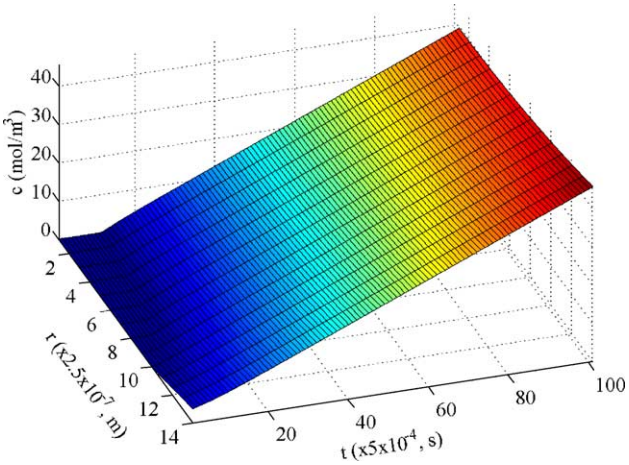

Fig. 4. 3D plot of Li/Li$^+$ concentration profile under a uniform and constant surface flux density injection. $J_o=0.001$ moles/m^2/s, $c_o=0$ moles/m^3.

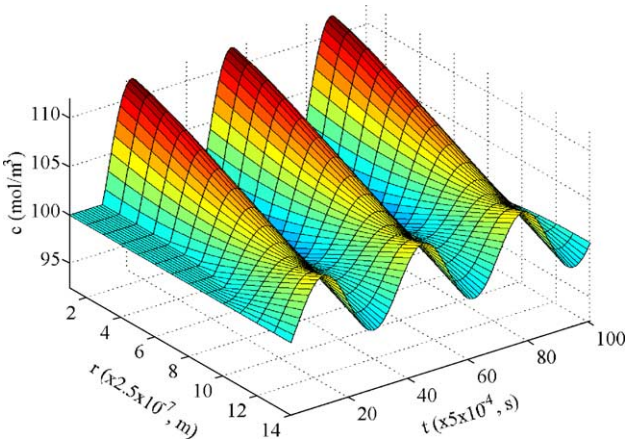

Fig. 5. 3D plot of Li/Li^+ concentration profile under a uniform and time-dependent surface flux density injection. $j_n(t) = -J_o\sin(\omega t)$ moles/m^2/s, $c_o = 100$ moles/m^3.

often subject to periodically changing and discharging. This is given as:

$$j_n(t) = -J_0\sin(\omega t)\left(\text{moles}/\text{m}^2/\text{s}\right). \tag{21}$$

Using (21) in (16), it immediately results:

$$\begin{aligned} c(r,t) = c_0 &+ \frac{3J_0}{\omega R_o}[1-\cos(\omega t)] \\ &- \frac{J_0\sin(\omega t)}{10DR_o}\left[3R_o^2 - 5r^2\right] - \frac{2R_oJ_0}{D} \\ &\times \sum_{m=1}^{\infty} \frac{\sqrt{1+\lambda_m^2}}{\lambda_m^3}\frac{\sin(\lambda_m r/R_o)}{r/R_o} \\ &\times \frac{1}{1+\left(\frac{\omega R_o^2}{\lambda_m^2 D}\right)^2}\left\{\frac{\omega R_o^2}{\lambda_m^2 D}\left[\cos(\omega t) - e^{-\lambda_m^2 Dt/R_o^2}\right]\right. \\ &\left. + \left(\frac{\omega R_o^2}{\lambda_m^2 D}\right)^2 \sin(\omega t)\right\} \end{aligned} \tag{22}$$

The 3D plot of Eq. (22) is illustrated in Fig. 5 for the case of $c_0 = 100$ moles/m^3, $J_o = 0.001$ moles/m^2/s, and $\omega = 377$ radians/s. As the surface flux oscillates, so does the concentration at each point inside the sphere. Because of a traveling diffusion front, the time for the peak concentration to occur at a particular point is delayed for sometime compared to the time of the correspondent peak surface flux. In particular, the concentration at the center of the sphere remains the initial value until about 6 ms, which is consistent with the estimation in the previous example. Within the sphere, the magnitude of the concentration at the center is the largest because of the characteristics of a one-dimensional radial diffusion process (inwardly or outwardly).

5. Discussion

As demonstrated, applying the FIT to a linear diffusion BVP has several advantages over other classical analytical methods, such as the variable separation and the Laplace transform. First of all, the procedure of the FIT to obtain the solution to a linear diffusion BVP is quite straightforward and systematic, whereas the variable separation method does not have a definite procedure to follow, and it is largely dependent upon person's experience and skills to reach the solution. Secondly, there is no inversion difficulty in the FIT, whereas it is not true for the Laplace transform method, especially with complicated function forms. Thirdly, there are no restrictions on the function forms of the boundary conditions and internal source, whereas using the variable separation or Laplace methods, analytical solutions can be obtained only for a limited number of cases. Lastly and importantly, Eq. (16) can be easily used and programmed for computer evaluation of the concentration profile point by point, thus achieving a great savings in the time effort compared to the FDM and FEM methods.

The solution (16) is applicable to a uniform and constant or time-varying surface flux condition, as illustrated by two examples in the previous section. In lithium ion batteries, the porous electrodes consist of a matrix of micro granules of carbon graphite, or those of cobalt oxide immersed in an electrolyte. Because the dimension of these granules is in the order of a few microns, much smaller than the dimension of the electrode width, it is appropriate to assume a uniform surface flux on a spherical particle. However, this assumption is clearly invalid if the size of the granule is large and comparable to the thickness of the electrode, in which case a non-uniform surface flux results due to a concentration distribution across the electrode width. In this case, BVP (1) must be re-formulated such that the dependence of the initial condition, the surface flux, and the concentration on the azimuthal angle θ and zenithal angle ϕ must be considered. Even so, the PSS approach still applies as demonstrated by Ölçer in his work [9,10].

It should be pointed out that the purpose of this work is to present an approach, FIT, for lithium ion battery modelling that has not been so far appeared in literatures. The work also successfully demonstrated several advantages of the FIT and PSS approach over other conventional analytical and numerical methods by applying the approach to the Li intercalation process. It is not the intention of this paper to present modelling for the entire battery, instead, only intercalation process within the granules is focused, which counts only part of our effort for the lithium ion battery modelling. Thus, it is understood that the charge and mass transport processes across the separator, along the solution phase within the electrodes, as well as heat transport are not considered in this work.

Finally, the author would like to point out that the treatment of Li/Li^+ intercalation processes in the present work is a simplified one. First of all, the simplification lies on largely the assumption that the reaction kinetics of intercalation within the granules is so fast that the process can be approximated as diffusion-limited. This assumption is well justified in the work by Doyle [2,3] and others [5–7], as BVP (1) appears in all their work. However, the surface reaction of the Butler-Volmer type is replaced by a linear boundary condition in the present work to demonstrate the FIT approach, but it will be included in the

future work. Secondly, the phase activity is ignored, since currently few experimental data are available to show that the phase change of lithium ions will cause any significant deviations from the single phase intercalation process. Thirdly, the surface passivation is not included for the moment. But, since it plays a crucial role in lithium ion battery life, the process of passivation will be considered in our complete lithium ion battery modelling.

6. Conclusion

A general solution to the Li/Li^+ insertion into a spherical granule of carbon or cobalt oxide immersed in a conductive electrolyte, as exists in a porous electrode, is obtained using the finite integral transform and the pseudo-steady state approach. The solution applies to arbitrary linear function forms for internal source and boundary conditions. For a constant and uniform surface flux density, the solution degenerates to a well-known Carslaw's result. The solution to a specific time-varying surface flux density condition, the sinusoidal injection, is also obtained. The results can be used for rapid and accurate modelling and simulation.

Nomenclature

A_m	norm
c	concentration distribution (moles/m^3)
c_0	initial concentration distribution (moles/m^3)
D	diffusion coefficient (m^2/s)
f_i	flux density on the ith coordinate surface (moles/m^2/s)
g	internal source (moles/m^3/s)
j_n	normal flux density (moles/m^2/s)
J_0	constant flux density (moles/m^2/s)
R^3	3-dimensional space
R_o	radius of spherical granule (m)
S_i	ith coordinate surface (m^2)
t	time (s)
V	volume (m^3)
v_d	diffusion velocity (m/s)

Greek letters

χ	normalized concentration distribution
χ_{0j}	zero-order pseudo-steady state
δ_{ij}	Kronecker operator
ϕ	zenith angle
λ_m	eigen value
θ	azimuthal angle
ρ	normalized radial coordinate
τ	normalized time
ψ_m	eigen function
Ω	domain
Ω_j	concentration function

Subscripts

0	Initial, or constant, or zero-order
i	1, 2, . . ., q
j	0, 1, . . ., q
m	1, 2, . . ., ∞
n	*normal*
q	number of pseudo-steady states

Acronyms

BVP	boundary value problem
FDM	finite difference method
FEM	finite element method
FIT	finite integral transform
Li/Li^+	lithium atom or ion
PSS	pseudo-steady state

Acknowledgement

The support of this work is provided by Dr. Roger Dougal's and Dr. Ralph White's grants from the U.S. National Reconnaissance Office under contract No. NRO 000-03-C-0122.

References

[1] J. Newman, Electrochemical Systems, 2nd ed., Prentice-Hall, Englewood Cliffs, New Jersey, 1991.
[2] M. Doyle, T.F. Fuller, J. Newman, J. Electrochem. Soc. 140 (1993) 1526.
[3] T.F. Fuller, M. Doyle, J. Newman, J. Elctrochem. Soc. 141 (1994) 1.
[4] D.A.G. Bruggeman, Ann. Phys. (Leipz.) 24 (1935) 636.
[5] P.M. Gomadam, J.W. Weidner, R.A. Dougal, R.E. White, J. Power Sources 110 (2002) 267.
[6] P. Ramadass, B. Haran, R.E. White, B.N. Popov, J. Power Sources 123 (2003) 230.
[7] G. Sikha, B.N. Popov, R.E. White, J. Electrochem. Soc. 151 (2004) A1104.
[8] M.N. Özişik, Boundary Value Problems of Heat Conduction, Dover Publications, Inc., New York, 1989.
[9] N.Y. Ölçer, Int. J. Heat Mass Transfer 7 (1964) 307.
[10] N.Y. Ölçer, Int. J. Heat Mass Transfer 8 (1965) 529.
[11] H.S. Carslaw, J.C. Jaeger, Conduction of Heat in Solids, Oxford University Press, London, 1959, p. 242.
[12] J.A. Bittencourt, Fundamentals of Plasma Physics, Pergamon Press, New York, 1986, p. 245.